Attenuation Measurement of Very Low Loss Dielectric Waveguides by the Cavity Resonator Method Applicable in the Millimeter/Submillimeter Wavelength Range

FRED I. SHIMABUKURO, MEMBER, IEEE, AND C. YEH, FELLOW, IEEE

Abstract—**A dielectric waveguide shorted at both ends is constructed as a cavity resonator. By measuring the Q of this cavity, one can determine the attenuation constant of the guided mode on this dielectric structure. The complex permittivity of the dielectric waveguide material can also be derived from the measurements. Measurements were made at *Ka*-band for dielectric waveguides constructed of nonpolar, low-loss polymers such as Teflon, polypropylene, polyethylene, polystyrene, and rexolite.**

I. Introduction

BY USING A specially configured dielectric rod made from low-loss, nonpolar polymers, one can construct millimeter/submillimeter dielectric waveguides supporting the dominant mode with a very small attenuation coefficient. To verify experimentally the low-loss characteristics of such waveguides, an accurate measurement scheme must be devised. A logical solution is the construction of a cavity consisting of a length of a dielectric rod waveguide supporting the mode of interest, with parallel shorting plates at both ends [1]. At a resonant frequency of such a cavity, the guide wavelength, λ_g, is obtained from the cavity spacing, and the attenuation constant, α, can be obtained from the measured Q. This cavity method also provides an accurate determination of the dielectric properties of the waveguide material.

This paper will first describe the theoretical foundation for this cavity technique. Then, a detailed discussion and derivation of the relationship between α and Q are given. Finally, experimental results for several low-loss dielectric materials are presented.

II. Theoretical Foundation

The geometry of a dielectric rod resonator, including a schematic of the measurement system, is shown in Fig. 1. The signals are coupled in and out of the resonator through small coupling holes in the center of the reflecting plates. For a circular step-index dielectric rod, the HE_{11} mode is the dominant guided mode for this dielectric waveguide [2], [3]. The longitudinal fields of this HE_{11} mode resonating between two shorting, parallel plates are, inside the core region ($\rho < a$),

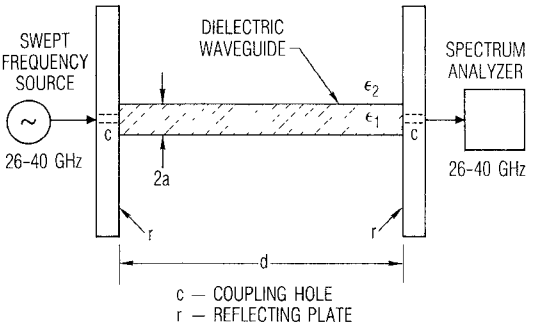

Fig. 1. The schematic of the dielectric waveguide cavity resonator, including measurement setup.

$$E_{zi} = AJ_1(u\rho)\sin\phi\cos\beta z \tag{1}$$

$$H_{zi} = BJ_1(u\rho)\cos\phi\sin\beta z \tag{2}$$

$$u^2 = k_1^2 - \beta^2 \qquad k_1^2 = \omega^2\mu\epsilon_1 \tag{3}$$

and

$$\beta = \frac{m\pi}{d}, \qquad m = 1,2,3\cdots.$$

Outside the core region ($\rho > a$), they are

$$E_{zo} = CK_1(w\rho)\sin\phi\cos\beta z \tag{4}$$

$$H_{zo} = DK_1(w\rho)\cos\phi\sin\beta z \tag{5}$$

with

$$w^2 = \beta^2 - k_2^2 \qquad k_2^2 = \omega^2\mu\epsilon_2. \tag{6}$$

In the previous equations, A, B, C, and D are arbitrary constants, $J_1(u\rho)$ is the Bessel function, $K_1(w\rho)$ is the modified Bessel function, a is the radius of the dielectric rod, d is the spacing between the shorting plates, ϵ_1 and ϵ_2 are the permittivities of the regions inside and outside the

Manuscript received August 13, 1987; revised January 30, 1988. This work was supported by the U.S. Air Force under Contract FO4701-87-C-0088 and by the UCLA–TRW Micro Program.

F. I. Shimabukuro is with the Aerospace Corporation, P.O. Box 92957, Los Angeles, CA 90009.

C. Yeh is with the Electrical Engineering Department, University of California at Los Angeles, Los Angeles, CA 90024.

IEEE Log Number 8821626.

0018-9480/88/0700-1160$01.00 ©1988 IEEE

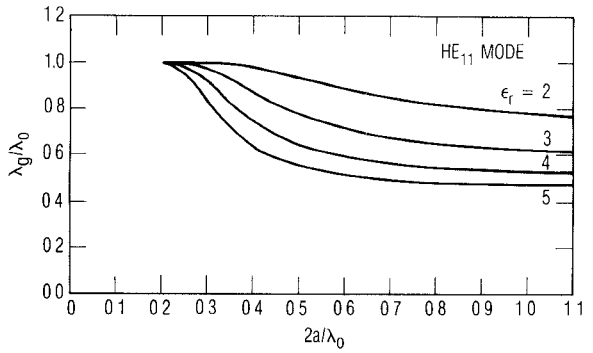

Fig. 2. Dispersion of the HE_{11} mode of a rod dielectric waveguide of radius a. The solution is given as a plot of the normalized guide wavelength as a function of normalized rod diameter. λ_0 is the free-space wavelength.

core, respectively, ω is the angular frequency of the resonant mode, and $\mu = \mu_0$ is the permeability of free space. In this study, the region outside the core is free space, and $\epsilon_2 = \epsilon_0$. It is noted that all transverse fields $(E_\phi, E_\rho, H_\phi, H_\rho)$, may be derived from the longitudinal fields, E_z and H_z [4]. By satisfying the boundary conditions at $\rho = a$, the following dispersion relation is obtained:

$$\left[\frac{J_1'(ua)}{uJ_1(ua)} + \frac{K_1'(wa)}{wK_1(wa)}\right]\left[\frac{k_1^2 J_1(ua)}{uJ_1(ua)} + \frac{k_0^2 K_1'(wa)}{wK_1(wa)}\right] = \left(\frac{\beta}{a}\right)^2\left[\frac{1}{u^2} + \frac{1}{w^2}\right]^2. \quad (7)$$

The solution of this dispersion relation will yield the guide wavelength, λ_g, of the cavity for the HE_{11} mode for given a, d, ϵ_1/ϵ_0, μ_0, and ω. Results for various values of ϵ_r $(= \epsilon_1/\epsilon_0)$ are shown in Fig. 2.

III. Ultrahigh Q Dielectric Rod Resonant Cavity

As shown in Fig. 1, a dielectric rod resonant cavity consists of a dielectric waveguide of length d terminated at its ends by sufficiently large, flat, and highly reflecting plates that are perpendicular to the axis of the guide. Microwave energy is coupled into and out of the resonator through small coupling holes at both ends of the cavity. For best results, the holes are dimensioned such that they are beyond cutoff. At resonance, the length of the cavity, d, must be $m\lambda_g/2$ (m an integer), where λ_g is the guide wavelength of the particular mode under consideration. By measuring the resonant frequency of the cavity, one may obtain the guide wavelength of that particular guided mode in the dielectric waveguide. The propagation constant, β, of that mode is related to λ_g and v_p, the phase velocity, as follows:

$$\beta = \frac{2\pi}{\lambda_g} = \frac{\omega}{v_p}. \quad (8)$$

The Q of a resonator is indicative of the energy storage capability of a structure relative to the associated energy dissipation arising from various loss mechanisms, such as those due to the imperfection of the dielectric material and the finite conductivity of the end plates. The common definition for Q is applicable to the dielectric rod resonator and is given by

$$Q = \omega \frac{\overline{W}}{\overline{P}} \quad (9)$$

where ω is the angular frequency of oscillation, $\overline{W}$ is the total time-averaged energy stored, and $\overline{P}$ is the average power loss.

For the case under study, with carefully machined dielectric rods and proper cavity alignment, the time-averaged power dissipation $\overline{P}$ consists of two parts, the power loss due to the dielectric rod and that due to the metal end walls, namely,

$$\overline{P} = \overline{P}_{\text{dielectric}} + \overline{P}_{\text{wall}}.$$

The power dissipation due to the dielectric rod is given by

$$\overline{P}_{\text{dielectric}} = \frac{1}{2}\sigma_d \int_0^d \int_{A_d} (\boldsymbol{E}_1 \cdot \boldsymbol{E}_1^*)\, dA\, dz \quad (10)$$

where $\boldsymbol{E}_1$ is the electric field within the dielectric rod, σ_d is the conductivity of the dielectric, A_d is the cross-sectional area of the dielectric rod, and the asterisk denotes the complex conjugate. The losses due to both end walls are given by

$$\overline{P}_{\text{wall}} = 2\left(\frac{R_s}{2}\right)\int_{A_w} (\boldsymbol{H}_t \cdot \boldsymbol{H}_t^*)\, dA \quad (11)$$

where $R_s = \sqrt{\omega\mu/2\sigma_r}$, the wall surface resistivity, σ_r is the conductivity of the reflector material, and $\boldsymbol{H}_t$ is the tangential component of the magnetic field along the metal wall. Here, A_w is the area of each conducting wall. There is also a loss due to the coupling hole, but, as in this experiment, the coupling can be made sufficiently small, such that the primary wall losses can be considered to be the ohmic wall losses:

$$\overline{W} = 2\overline{W}_m = 2\overline{W}_e = \mu\int_V (\boldsymbol{H}\cdot\boldsymbol{H}^*)\, dV = \epsilon\int_V (\boldsymbol{E}\cdot\boldsymbol{E}^*)\, dV \quad (12)$$

where V is the total volume of the cavity, $\overline{W}_m$ and $\overline{W}_e$ are the time-averaged magnetic and electric energies, respectively, and $\boldsymbol{H}$ and $\boldsymbol{E}$ are the total fields. Equation (9)–(12) can be rearranged to obtain

$$\frac{1}{Q} = \frac{\overline{P}}{\omega\overline{W}} = \frac{\overline{P}_{\text{dielectric}}}{\omega\overline{W}} + \frac{\overline{P}_{\text{wall}}}{\omega\overline{W}} = \frac{1}{Q_d} + \frac{1}{Q_w}. \quad (13)$$

The term Q_d is the Q factor of the cavity if the end plates were perfectly conducting, and Q_w is the Q factor of the cavity if the dielectric were perfect. From (13) we have

$$Q_d = \frac{\omega\overline{W}}{\overline{P}_{\text{dielectric}}} = \frac{1}{2\tan\delta\dfrac{\epsilon_1}{\epsilon_0}}\frac{C_T}{C_D} \quad (14)$$

$$Q_W = \frac{\omega\overline{W}}{\overline{P}_{\text{wall}}} = \frac{d}{2\delta_r}\frac{C_T}{C_W} \quad (15)$$

where $\tan\delta$ ($=\sigma/\omega\epsilon_1$) is the loss tangent of the dielectric rod, and δ_r ($=2R_s/\omega\mu$) is the skin depth of the metallic end plates. The ratios C_T/C_D and C_T/C_W are dimensionless quantities involving integrals of the fields.

It is noted that Q_d is independent of the length of the cavity whereas Q_w is proportional to the length. For a long cavity, $Q_w \gg Q_d$, and $Q \approx Q_d$. By measuring the Q of the cavity with $Q_w \gg Q_d$, one can obtain the attenuation constant α of the given mode.

In 1944 Davidson and Simmonds [5] derived a relation between the Q of a cavity composed of a uniform transmission line with short-circuiting ends, and the attenuation constant α of such a transmission line. Later, in 1950, Barlow and Cullen [6] rederived this relation. These authors showed that this relation is quite general and is applicable to uniform metal tube waveguides with arbitrary cross section. Since then, one of the standard techniques for the measurement of the attenuation constant α is the use of the cavity method.[1] This method offers an excellent way of measuring the attenuation constant of the guide when the loss is quite small. Later on this method was generalized and applied to open waveguides, such as the single wire line, the dielectric cylinder guide, and associated guides, by various authors, e.g., [1], [7].

However, it should be remembered that the formula by Davidson and Simmonds and Barlow and Cullen is derived under the assumption that there exists a single equivalent transmission line for the mode under consideration. This assumption is true for a pure TE, TM or TEM mode, but it is not clear that such a single equivalent transmission line exists for the hybrid waves. This suspicion arises from the fact that a) the TE and TM waves are intimately coupled to each other, and b) the characteristic impedance defined by Schelkunoff [8] is not constant with respect to the transverse coordinates. It is, therefore, very difficult to conceive the possibility that there exists a single equivalent transmission line for this hybrid mode; at best the hybrid wave may be represented by a set of transmission lines coupled tightly with one another. Hence, the formula by Davidson and Simmonds and Barlow and Cullen is *not* applicable to the hybrid wave.[2]

A more general relation between Q and α can be obtained without using the transmission line equivalent circuit, provided that α is very small compared with β. The propagation constant of a guided wave with small attenuation constant at ω is

$$\Gamma(\omega) = \alpha(\omega) + j\beta(\omega), \qquad j=\sqrt{-1}. \tag{16}$$

It can be shown that for a waveguide placed between reflecting parallel plates, with minuscule coupling to external circuits,

$$P_t \sim \frac{1}{|1 - r^2 \exp(-2\Gamma d)|^2} \tag{17}$$

where P_t is the power transmission of the resonator, r is the reflection coefficient at each wall, Γ is the propagation constant, given in (16), and d is the distance between the reflecting plates. At the half-power transmission points,

$$P_t(\omega = \omega_0) = 2P_t(\omega = \omega_0 \pm \Delta\omega) \tag{18}$$

and

$$\beta = \beta_0 + \Delta\beta$$
$$\alpha = \alpha_0 + \Delta\alpha. \tag{19}$$

For the case $r=1$ and $\alpha d \ll 1$, and using (17)–(19), one gets

$$\Delta\beta = \alpha. \tag{20}$$

Since

$$\Delta\beta \approx \frac{\partial\beta}{\partial\omega}\Delta\omega \qquad v_p = \frac{\omega}{\beta} \qquad v_g = \frac{\partial\omega}{\partial\beta}$$

and

$$Q = \frac{\omega_0}{2\,\Delta\omega}$$

we finally arrive at the relation

$$\alpha = \frac{\omega_0}{2Qv_g} = \frac{v_p}{v_g}\frac{\beta}{2Q}. \tag{21}$$

This is the general relation that we are seeking. This result was also obtained by Yeh [9] using an alternative approach. Substituting the values of v_p/v_g for TE, TM or TEM into (21), one gets the relations derived by Davidson *et al.* For the TM or TE mode,

$$\frac{v_p}{v_g} = \frac{1}{1-\left(\frac{\lambda}{\lambda_c}\right)^2} \qquad \alpha = \frac{1}{1-\left(\frac{\lambda}{\lambda_c}\right)^2}\frac{\beta}{2Q}$$

and for the TEM mode,

$$v_p/v_g = 1 \qquad \alpha = \beta/2Q$$

where λ_c is the cutoff wavelength.

The group and phase velocity of the dominant modes can be obtained easily from the $\omega-\beta$ diagram. A sketch of the $\omega-\beta$ diagram for the propagating modes is shown in Fig. 3. It can be seen that at low frequencies or small β's, $v_p \approx v_g$ and again at very high frequencies or large β's, $v_p \approx v_g$. Therefore, the relation $\alpha = \beta/2Q$ is applicable only at very low frequencies or at very high frequencies.

Returning now to the problem of measuring the attenuation constant of very low loss dielectric waveguides, one notes that using the dielectric waveguide cavity technique, a Q of the order of 30000 can readily be measured. At the higher frequencies this value of Q corresponds to a loss tangent of the order of 10^{-5}. A schematic of the experiment is shown in Fig. 1. A dielectric rod waveguide is

[1] The procedures of this method in general are the following: Short-circuit the uniform transmission line under consideration at both ends and measure the Q of such a resonator. From the knowledge of the measured Q and other constants, such as the cutoff frequency of the guide and the frequency of oscillation, it is an easy matter to obtain from the formula derived by these authors.

[2] But several investigators, apparently unaware of this restriction, used this formula in their investigations of the hybrid wave.

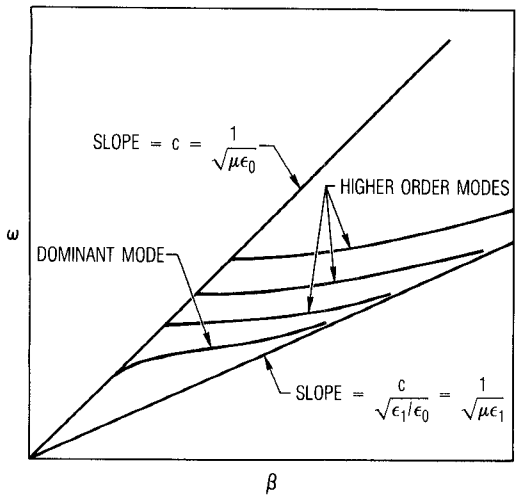

Fig. 3. Sketch of the $\omega-\beta$ diagram for several propagating modes along a dielectric waveguide.

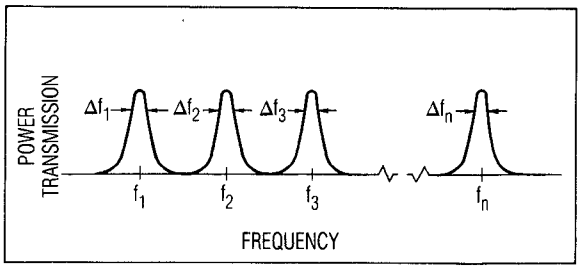

Fig. 4. Power output of a swept input signal through a dielectric waveguide in a parallel-plate resonator.

placed in a parallel-plate cavity, and a swept signal frequency is transmitted through the waveguide cavity and detected by a spectrum analyzer. The signals are coupled through very small holes in the circular gold plated reflectors. The plates are large enough (6 in. diameter) such that the fields beyond the plate diameter are insignificant. The output is a series of narrow transmission resonances at $f_1, f_2, \cdots, f_m$ with half-power bandwidths, $\Delta f_1, \Delta f_2, \cdots, \Delta f_m$, respectively (see Fig. 4). At each resonant frequency the guide wavelength is given by

$$\lambda_{gm} = \frac{2d}{m} \tag{22}$$

and the Q by

$$Q_m = \frac{f_m}{\Delta f_m} \tag{23}$$

where d is the length of the waveguide and m is the mth resonance. The integer m is the number of guide half-wavelengths at a particular resonant frequency. From a, the dielectric rod radius, the spacing d, the guide wavelength λ_g, and the number m, the relative dielectric constant, $\epsilon_r = \epsilon_1/\epsilon_0$, can be determined at the different frequencies using the solutions of (7).

With careful alignment of the waveguide and the shorting plates the primary loss mechanisms to be considered are the wall losses and the dielectric loss. From previous

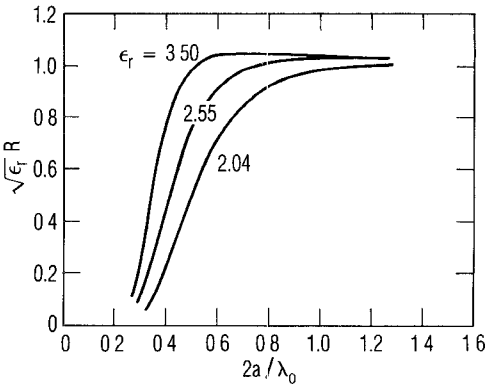

Fig. 5. Plots of the attenuation factor R in a circular dielectric waveguide of radius a for different relative permittivities.

discussion,

$$\frac{1}{Q_m} = \frac{1}{Q_d} + \frac{1}{Q_w} \tag{24}$$

where Q_m is the measured Q of the mth mode, recalling that Q_d is independent of cavity length, whereas Q_w is proportional to the cavity length. For the different dielectric waveguides used in this study, the calculated Q_w ranges from 18000 to 21000 d, where d is the length in cm. Experimentally, the effect of the wall losses, whether due to the coupling or to the ohmic dissipation, on the cavity Q could not be detected; therefore,

$$Q_w \gg Q_d. \tag{25}$$

The measurement verification of (25) will be discussed in the next section.

The general relation between Q and α for a short-circuited low-loss waveguide given in (21) is rewritten as

$$\alpha = 8.686 \frac{v_p}{v_g} \frac{\beta}{2Q} \quad \text{dB/m} \tag{26}$$

where $v_p = \omega/\beta$ and $v_g = d\omega/d\beta$. It has been shown that, for a dielectric rod waveguide [10],

$$\alpha = 4.343\omega\sqrt{u\epsilon_0}\tan\delta\epsilon_r R \tag{27}$$

where

$$R = \left| \frac{\int_{A_d} (\boldsymbol{E}_1 \cdot \boldsymbol{E}_1^*)\, dA}{\sqrt{\frac{\mu}{\epsilon_0}} \int_A \boldsymbol{e}_z \cdot (\boldsymbol{E} \times \boldsymbol{H}^*)\, dA} \right|. \tag{28}$$

As before $\epsilon_r = \epsilon_1/\epsilon_0$, A_d is the cross-sectional area of the core region of the dielectric waveguide, A is the total cross-sectional area, $\boldsymbol{E}_1$ is the electric field within the dielectric rod, $\boldsymbol{e}_z$ is the unit vector along the direction of propagation, and $\boldsymbol{E}$ and $\boldsymbol{H}$ are the total fields. The quantity R is a frequency-dependent geometrical factor which can be computed. The loss tangent can be obtained

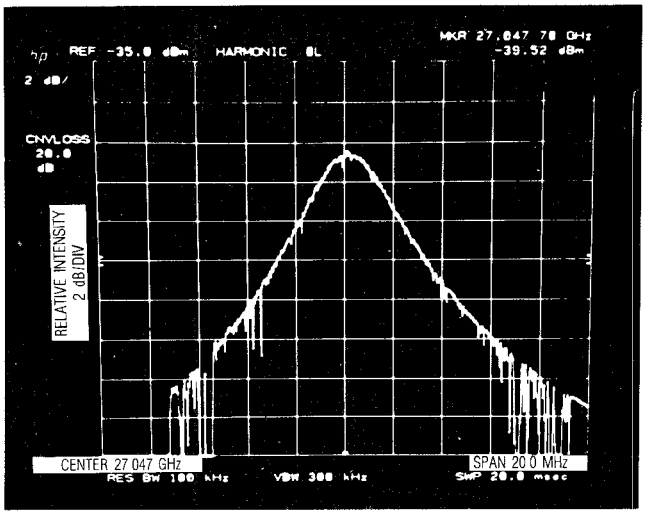

Fig. 6. Photograph of the output on the spectrum analyzer through the dielectric waveguide in the parallel-plate cavity at a transmission resonance.

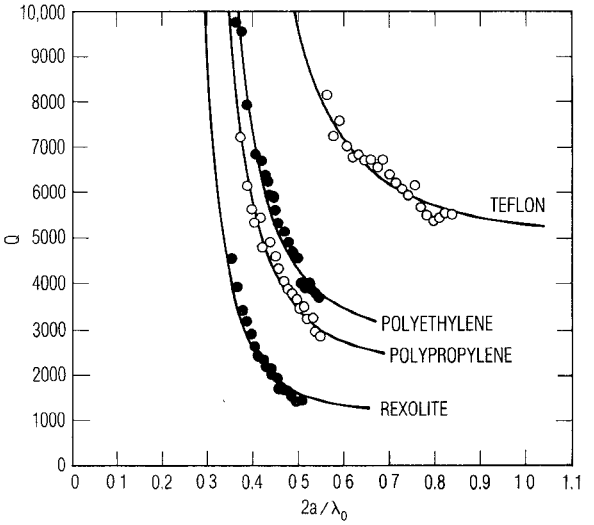

Fig. 7. Measured Q's of the different circular dielectric waveguides. The solid line is the theoretical Q_d curve using the permittivities given in Table I.

by combining (26) and (27):

$$\tan\delta = \frac{\frac{v_p}{v_g}\frac{\beta}{Q}}{\omega\sqrt{\mu\epsilon_0}\epsilon_r R}. \tag{29}$$

For a circular dielectric waveguide, one can calculate R for different values of ϵ_r. This is shown in Fig. 5. Hence, by measuring the Q of a dielectric rod in a parallel-plate resonator, the loss tangent of the dielectric and the attenuation constant for the corresponding mode can be obtained. This scheme provides an extremely accurate way of measuring the electrical properties ($\epsilon_r, \tan\delta$) of ultra-low-loss dielectrics as well as the low attenuation constant for a dielectric waveguide supporing the dominant mode.

III. Experimental Results

Circular dielectric rod waveguides were made of Teflon, rexolite, polystyrene, polyethylene, and polypropylene. The diameters ranged from 0.4 to 0.63 cm, and the lengths from 15.2 to 20.3 cm. These waveguides were placed in a parallel-plate resonator. A swept frequency signal at *Ka*-band (26.5–40 GHz) was coupled into the resonator and the output was detected by a spectrum analyzer. The input and output coupling was done through a small hole (1.5 mm diam.) in an iris in WR-28 waveguide. With this coupling, only the HE_{11} dominant mode was excited. This was verified by mapping the fields outside the dielectric waveguide with an electric probe. A sample measurement of the transmission resonance on the spectrum analyzer is shown in Fig. 6, for a Teflon rod waveguide.

At each resonance the Q is measured. The results are shown in Fig. 7. Because m is known to be an integer it can be readily determined by measuring the guide wavelength approximately with a probe. Once m is known, the guide wavelengths at the various resonant frequencies are accurately determined, and the $\omega-\beta$ diagram can be generated, and α can be determined from (26). In this investigation the dielectric waveguides had a circular cross section and the following procedure was utilized. Once the guide wavelength and the waveguide dimensions were known, ϵ_r was determined from (7). Assuming the value of ϵ_r for Teflon in Table I, v_p and v_g can be calculated from (7), for a rod diameter of 0.635 cm. The comparison between the calculated and measured values of v_p and v_g is shown in Fig. 8. The measured group velocity was obtained by assuming a linear relation between adjacent measured values on the $\omega-\beta$ curve. The attentuation coefficient was calculated from (26) and $\tan\delta$ was obtained from (29). For the circular waveguide, the field

TABLE I
Measured Relative Permittivities and Loss Tangents, *Ka*-Band

Material	Estimates with Standard Error	
	ϵ_r	$10^3 \tan\delta$
Teflon	2.0422 ±0.0006	0.217 ±0.006
Polypropylene	2.261 ±0.001	0.50 ±0.03
Polyethylene	2.302 ±0.003	0.38 ±0.02
Polystyrene	2.542 ±0.001	0.87 ±0.07
Rexolite	2.548 ±0.001	0.89 ±0.07

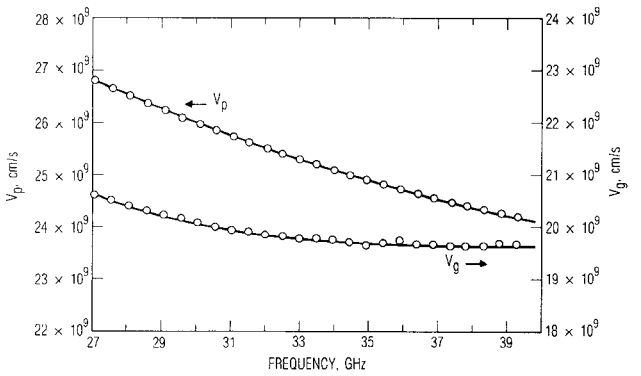

Fig. 8. Comparison of measured and calculated group and phase velocities for a Teflon rod waveguide of diameter 0.635 cm. The solid lines are calculated and the measurements are indicated by circles.

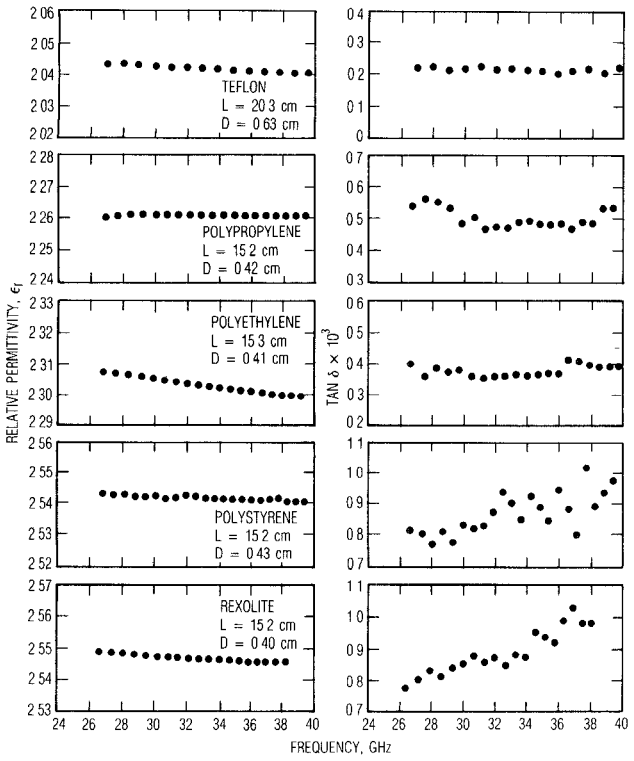

Fig. 9. Derived values of ϵ_r and $\tan\delta$ from the measurements for different dielectric materials.

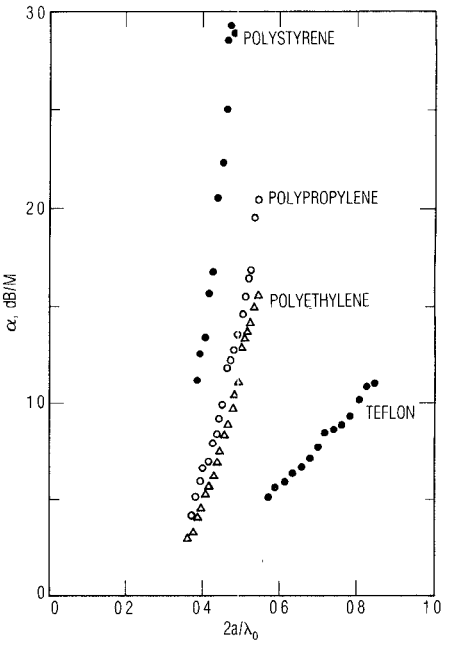

Fig. 10. Measured attenuation coefficients for the different dielectric waveguides corresponding to Fig. 8. Polystyrene and rexolite have similar attenuation characteristics.

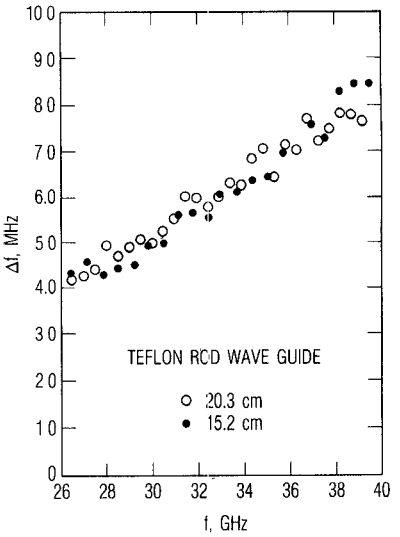

Fig. 11. Plot of half-power transmission bandwidths at the different resonances for two different lengths (6 in. and 8 in.) for circular Teflon waveguides.

configurations were known, and $\tan\delta$ was also calculated from (14), giving the same results as (29).

The measured relative permittivities and loss tangents at different resonant frequencies for the materials above are shown in Fig. 9. The average values with the corresponding standard deviations are given in Table I. A brief discussion, including references, of alternate methods used to determine the complex permittivities of materials at the millimeter wavelengths has been given in [11] and [12]. The corresponding attenuation coefficients for these dielectric waveguides are shown in Fig. 10. In Fig. 11 are shown plots of the half-power bandwidths at the different resonances for two lengths of 0.635-cm-diameter Teflon waveguide. The plot indicates that the measured Q's are primarily due to the dielectric losses. If the wall losses were significant, the Q's of the shorter length waveguide would have been noticeably lower at the lower frequencies and the derived loss tangents in Fig. 9 would have been noticeably higher. As a further check on the coupling effects, the insertion losses of the resonator system with a Teflon waveguide were measured at resonances near 27, 33, and 39 GHz. The measured insertion losses were -71 dB, -63 dB, and -51 dB, respectively, at these three frequencies.

It is clear that for low-loss performance in circular dielectric waveguides, one should use small-diameter rods made from material with small relative permittivity and loss tangent. At the *Ka*-band the attenuation in a dielectric rod waveguide for small $2a/\lambda_0$ can be less than that of a conventional rectangular metallic waveguide. Because the surface resistivity of metals is proportional to the square root of frequency, the losses of metallic waveguides increase with frequency relative to that of a dielectric waveguide. This is shown in Fig. 12. The attenuation coefficients of different silver rectangular waveguides and of circular Teflon waveguides at the indicated frequencies are plotted in the figure. The assumption is that for the Teflon rod, $2a/\lambda_0 = 0.4$ at the indicated frequencies. Since the attenuation coefficient of the dielectric waveguide can be further reduced by using other than a circular cross section, dielectrics show promise as viable guiding structures at the millimeter and submillimeter wavelengths.

To summarize, a resonator method applicable at the millimeter and submillimeter wavelengths which can accurately measure the attenuation coefficient of ultra-low-loss

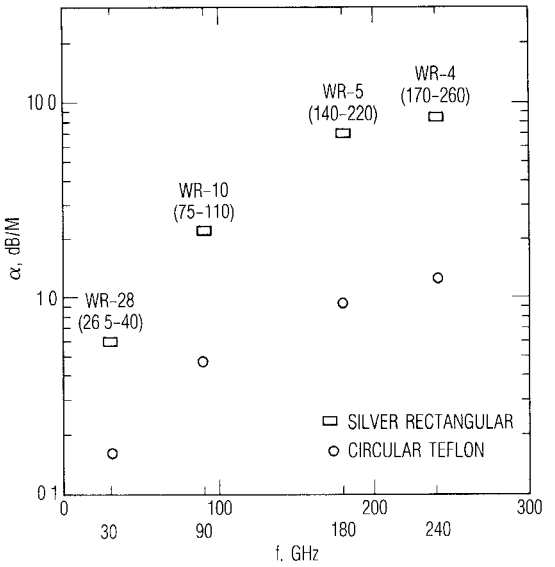

Fig. 12. Comparison of attenuation coefficients of silver rectangular and Teflon circular waveguides at the indicated frequencies. The waveguide range of the designated metal waveguides are shown in parentheses. For the dielectric waveguide, it is assumed that $2a/\lambda_0 = 0.4$ at the indicated frequencies

dielectric waveguides has been described. In addition, the complex permittivity of the dielectric material of the waveguide can be derived. Since the fields are confined close to the dielectric core, long resonators can be conveniently implemented, permitting accurate measurements of α, ϵ_r, and $\tan\delta$.

ACKNOWLEDGMENT

The authors wish to thank H. B. Dyson for his invaluable help in setting up the experiment and making the measurements, and G. G. Berry for fabricating the Fabry–Perot plates and dielectric waveguides. One of the authors (C. Y.) wishes to thank Dr. J. Hamada and Dr. B. Wong for their enthusiastic support of the UCLA–TRW MICRO Program.

REFERENCES

[1] C. Chandler, "Investigation of dielectric rod as waveguides," *J. Appl. Phys.*, vol. 20, pp. 1188–1192, 1949.

[2] J. R. Carson, S. P. Mead, and S. A. Schelkunoff, "Hyper-frequency waveguides—Mathematical theory," *Bell Syst. Tech. J.*, vol. 15, pp. 310–333, 1936.

[3] C. Yeh, "Advances in communication through light fibers," in *Advances in Communication Systems*, vol. 4, A. Viterbi, Ed. New York: Academic Press, 1975.

[4] S. Ramo, J. R. Whinnery, and T. Van Duzer, *Fields and Waves in Communication Electronics*, 2nd ed. New York: Wiley, 1984.

[5] C. F. Davidson and J. C. Simmonds, "Cylindrical cavity resonators," *Wireless Eng.*, vol. 31, pp. 420–424, 1944.

[6] H. M. Barlow and A. L. Cullen, *Microwave Measurements*. London: Constable and Co., 1950.

[7] D. D. King and S. P. Schlesinger, "Losses in dielectric image lines," *IRE Trans. Microwave Theory Tech.*, vol. MTT-5, pp. 31–35, 1957.

[8] S. A. Schelkunoff, "The impedance concept and its application to problems of reflection refraction, shielding and power absorption," *Bell Syst. Tech. J.*, vol. 17, pp. 17–48, 1938.

[9] C. Yeh, "A relation between α and Q," *Proc. IRE*, vol. 50, p. 2143, 1962.

[10] C. Yeh, "Attenuation in a dielectric elliptical cylinder," *IEEE Trans. Antennas Propagat.*, vol. AP-11, pp. 177–184, 1963.

[11] M. N. Afsar, "Dielectric measurements of millimeter wave materials," *IEEE Trans. Microwave Theory Tech.*, vol. MTT-32, pp. 1598–1609, 1984.

[12] F. I. Shimabukuro, S. Lazar, M. R. Chernick, and H. B. Dyson, "A quasi-optical method for measuring the complex permittivity of materials," *IEEE Trans. Microwave Theory Tech.*, vol. MTT-32, pp. 659–665, 1984.

Fred I. Shimabukuro (M'56) was born in Honolulu, HI, on September 3, 1932. He received the B.S. and M.S. degrees in electrical engineering from M.I.T., Cambridge, MA, in 1955 and 1956, respectively, and the Ph.D degree from the California Institute of Technology, Pasadena, CA, in 1962.

He worked at the Hughes Aircraft Company from 1956 to 1958, and since 1962 has been employed at the Aerospace Corporation in El Segundo, CA. His current research activity is in millimeter and submillimeter wave technology.

Dr. Shimabukuro is a member of Sigma Xi.

C. Yeh (S'56–M'63–SM'82–F'85) was born in Nanking, China, on August 11, 1936. He received the B.S., M.S., and Ph.D. degrees in electrical engineering from the California Institute of Technology, Pasadena, CA, in 1957, 1958, and 1962, respectively.

He is presently Professor of Electrical Engineering at the University of California at Los Angeles (UCLA). He joined UCLA in 1967 after serving on the faculty of USC from 1962 to 1967. His current areas of research interest are optical and millimeter-wave guiding structures, gigabit-rate fiber-optic local area networks, and scattering of electromagnetic waves by penetrable, irregularly shaped objects.

Dr. Yeh is a member of Eta Kappa Nu, Sigma Xi, and the Optical Society of America.